

Hydrogen production by steam reforming of LNG over Ni/Al₂O₃–ZrO₂ catalysts: Effect of Al₂O₃–ZrO₂ supports prepared by a grafting method

Jeong Gil Seo, Min Hye Youn, In Kyu Song*

*School of Chemical and Biological Engineering, Research Center for Energy Conversion and Storage,
Seoul National University, Shinlim-dong, Kwanak-ku, Seoul 151-744, South Korea*

Received 24 October 2006; received in revised form 2 December 2006; accepted 4 December 2006
Available online 9 December 2006

Abstract

Al₂O₃–ZrO₂ supports with various zirconium contents were prepared by grafting a zirconium precursor onto the surface of γ -Al₂O₃. Ni(20 wt%)/Al₂O₃–ZrO₂ catalysts were then prepared by an impregnation method, and were applied to the hydrogen production by steam reforming of LNG. The effect of Al₂O₃–ZrO₂ supports on the performance of the Ni(20 wt%)/Al₂O₃–ZrO₂ catalysts was investigated. Al₂O₃–ZrO₂ prepared by a grafting method served as an efficient support for the nickel catalyst in the steam reforming of LNG. ZrO₂ inhibited the incorporation of nickel species into the lattice of Al₂O₃ and prevented the growth of metallic nickel particles during the reduction step. The crystalline structures and catalytic activities of the Ni(20 wt%)/ZrO₂–Al₂O₃ catalysts were strongly influenced by the amount of zirconium grafted. LNG conversion and hydrogen yield showed volcano-shaped curves with respect to zirconium content. Among the catalysts tested, the Ni(20 wt%)/ZrO₂–Al₂O₃ (Zr/Al = 0.17) catalyst showed the best catalytic performance in terms of both LNG conversion and hydrogen yield. The well-developed and pure tetragonal phase of ZrO₂–Al₂O₃ (Zr/Al = 0.17) played an important role in the adsorption of steam and the subsequent spillover of steam from the support to the active nickel. The high reducibility of Ni(20 wt%)/ZrO₂–Al₂O₃ (Zr/Al = 0.17) was also responsible for the enhanced performance of the catalyst.

© 2006 Elsevier B.V. All rights reserved.

Keywords: Alumina–zirconia support; Nickel catalyst; Grafting method; LNG; Steam reforming; Hydrogen production

1. Introduction

Catalytic reforming technology of methane has been widely studied for use in the large-scale production of hydrogen or carbon monoxide [1–4]. In particular, steam reforming of methane is generally accepted as a feasible route to produce hydrogen for various fuel cell systems [5–7]. Liquefied natural gas (LNG), which is abundant and mainly composed of methane, can serve as an alternate source for hydrogen production by steam reforming. The extensive piping system for LNG in modern cities also makes LNG well suited as a hydrogen source for residential reformers.

Nickel-based catalysts have been widely used in the steam reforming reactions. However, the nickel-based catalysts require a high reaction temperature and excess amount of steam to prevent the coke deposition on the catalyst surfaces [1,3]. Sup-

ported nickel catalysts generally suffer from severe catalyst deactivation due to the sintering of nickel particles [7] and the insufficient thermal and chemical stability of the support [8]. Several attempts have been made to overcome these problems. These examples include the addition of second metals such as potassium, magnesium, cerium, and molybdenum [9–12], and the impregnation of nickel catalyst on various supports such as ZrO₂, SiO₂, and mixed oxides [13–15].

It is well known that the performance of a supported nickel catalyst depends, not only on the nature and structure of the active nickel, but also on the chemical and textural property of the support. The selection and modification of an appropriate support for a nickel catalyst, therefore, can be a potential route to improve the catalytic performance of a supported nickel catalyst. It has been reported that zirconia support enhanced the adsorption of steam onto its surface and activated the gasification of hydrocarbons or carbon precursors adsorbed on the catalyst surface in the steam reforming reactions, resulting in an enhancement in hydrogen yield and coke resistance [16]. In the steam and CO₂ reforming of methane, Ni/ZrO₂ was found to show a

* Corresponding author. Tel.: +82 2 880 9227; fax: +82 2 889 7415.
E-mail address: inksong@snu.ac.kr (I.K. Song).

higher catalytic activity and long-term stability than Ni/Al₂O₃ catalyst [17]. It was also reported that Pt/Al₂O₃–ZrO₂ catalyst showed a better activity and higher stability than Pt/Al₂O₃ catalyst in the production of synthesis gas by dry reforming of methane [18]. Furthermore, Ni/Al₂O₃–ZrO₂ catalyst showed a high activity and strong resistance to coke deposition in the partial oxidation and dry reforming of methane [19]. However, no attempt has been made to utilize an Al₂O₃–ZrO₂ support for nickel catalysts in the hydrogen production by steam reforming of LNG.

Al₂O₃–ZrO₂ can be synthesized by co-precipitation [20], sol–gel [21], and grafting methods [22–24]. Alumina, which has many hydroxyl groups on the surface, can be modified by grafting a zirconium precursor onto the surface of alumina. The chemical properties of Al₂O₃–ZrO₂ prepared by a grafting method are different from those of Al₂O₃–ZrO₂ prepared by a co-precipitation method or a sol–gel method [22]. Therefore, it is expected that Al₂O₃–ZrO₂ prepared by a grafting method would show interesting properties as a support for nickel catalyst.

In this work, a series of Al₂O₃–ZrO₂ supports with various zirconium loadings were prepared by grafting a zirconium precursor onto the surface of γ -Al₂O₃. Ni/Al₂O₃–ZrO₂ catalysts were then prepared by an impregnation method for use in the hydrogen production by steam reforming of LNG. The effect of Al₂O₃–ZrO₂ supports on the performance of Ni/Al₂O₃–ZrO₂ catalysts in the steam reforming of LNG was investigated.

2. Experimental

2.1. Preparation of Al₂O₃–ZrO₂ (AZ-X) support and Ni/Al₂O₃–ZrO₂ (Ni/AZ-X) catalyst

Al₂O₃–ZrO₂ supports with various zirconium loadings were prepared by grafting an appropriate amount of zirconium precursor onto the surface of γ -Al₂O₃, according to the similar method reported in literatures [22–24]. Fig. 1 shows the schematic procedure for the preparation of Al₂O₃–ZrO₂ support by a grafting method. A known amount of alumina (γ -Al₂O₃, Degussa) was added to 100 ml of anhydrous toluene (Aldrich) for uniform dispersion, and an excess amount of triethylamine (TEA, Fluka) was then added to the alumina slurry to activate the hydroxyl groups on the alumina surface. An appropriate amount of zirconium precursor (Zr(OBu)₄, Aldrich) was slowly added to the slurry with constant stirring for 1 h, and the resulting slurry was

stirred at room temperature for 6 h to achieve the complete reaction of the activated surface hydroxyl groups of alumina with butoxide groups of the zirconium precursors. After removing the unreacted zirconium precursor and butanol (by-product) by centrifugation, the slurry was washed several times with anhydrous toluene. Upon the addition of an excess amount of deionized water to the washed slurry, a white gel was formed within a few seconds. After maintaining the white gel in deionized water for 6 h, a solid product was obtained by filtration. The solid product was dried overnight at 120 °C, and then calcined at 700 °C for 5 h to yield the Al₂O₃–ZrO₂ support. The prepared Al₂O₃–ZrO₂ support was denoted as AZ-X (X = 1–4), where X is the number of times the whole preparation process was repeated. For example, AZ-2 denotes an Al₂O₃–ZrO₂ support that was prepared by repeating the entire process two times (by adding known amounts of Zr(OBu)₄ two times through the entire preparation process).

Ni/Al₂O₃–ZrO₂ catalysts were prepared by impregnating known amounts of a nickel precursor (Ni(NO₃)₂•6H₂O, Aldrich) onto γ -Al₂O₃ (AZ-0), AZ-1, AZ-2, AZ-3, and AZ-4 supports. The nickel loading was fixed at 20 wt% in all cases. The prepared catalysts were denoted as 20Ni/AZ-X (X = 0–4).

2.2. Characterization

The chemical compositions of Al₂O₃–ZrO₂ (AZ-X) supports were determined by ICP-AES analyses (ICPS-1000IV, Shimadzu). The crystalline phases of supports and supported catalysts were investigated by XRD (M18XHF-SRA, MAC Science) measurements using Cu-K α radiation ($\lambda = 1.54056 \text{ \AA}$) operated at 50 kV and 100 mA. In order to examine the reducibility of supported catalysts, temperature-programmed reduction (TPR) measurements were carried out in a conventional flow system with a moisture trap connected to a thermal conductivity detector (TCD) at temperatures ranging from room temperature to 1000 °C with a ramping rate of 5 °C/min. For the TPR measurements, a mixed stream of H₂ (2 ml/min) and N₂ (20 ml/min) was used for 0.1 g of catalyst sample.

2.3. Steam reforming of LNG

The steam reforming of LNG was carried out in a continuous flow fixed-bed reactor at atmospheric pressure. Each calcined catalyst (100 mg) was charged into a tubular quartz reactor, and it was then reduced with a mixed stream of H₂ (10 ml/min) and N₂ (30 ml/min) at 800 °C for 3 h. Water was sufficiently vaporized by passing a pre-heating zone and continuously fed into the reactor together with LNG (92.0 vol.% of CH₄ and 8.0 vol.% of C₂H₆) and N₂ carrier (30 ml/min). The steam/carbon ratio in the feed stream was fixed at 2.0, and the total feed rate with respect to the catalyst was maintained at 27,000 ml h⁻¹/g. The catalytic reaction was carried out at 600 °C. The reaction products were periodically sampled and analyzed using an on-line gas chromatograph (Younglin, ACME 6000) equipped with a thermal conductivity detector. LNG conversion and hydrogen yield were calculated according to the following equations on

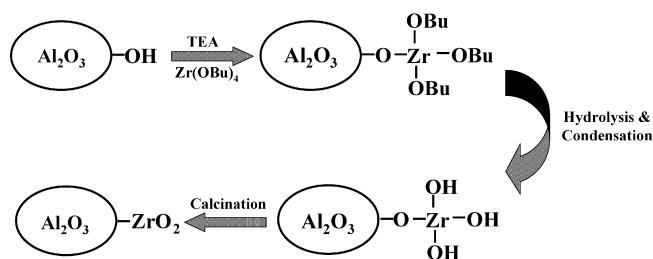


Fig. 1. Schematic procedure for the preparation of Al₂O₃–ZrO₂ support by a grafting method.

Table 1
Chemical compositions of Al₂O₃–ZrO₂ (AZ-X) supports determined by ICP-AES analyses

| Support | Amount of Zr used (wt%) | Zr loading (wt%) | Zr/Al atomic ratio |
|---------|-------------------------|------------------|--------------------|
| AZ-1 | 15 | 13.4 | 0.09 |
| AZ-2 | 30 | 21.9 | 0.17 |
| AZ-3 | 45 | 31.8 | 0.31 |
| AZ-4 | 60 | 38.4 | 0.45 |

the basis of carbon balance:

$$\text{LNG conversion (\%)} = \left(1 - \frac{F_{\text{CH}_4, \text{out}} + F_{\text{C}_2\text{H}_6, \text{out}}}{F_{\text{CH}_4, \text{in}} + F_{\text{C}_2\text{H}_6, \text{in}}} \right) \times 100,$$

$$\text{hydrogen yield (\%)} = \frac{F_{\text{hydrogen, out}}}{2F_{\text{CH}_4, \text{in}} + 3F_{\text{C}_2\text{H}_6, \text{in}}} \times 100$$

3. Results and discussion

3.1. Crystalline structure of AZ-X (X = 0–4)

Chemical compositions of Al₂O₃–ZrO₂ (AZ-X) supports determined by ICP-AES analyses are listed in Table 1. The amount of zirconium grafted onto γ -Al₂O₃ was increased with increasing amounts of zirconium used from AZ-1 to AZ-4. Although the amount of actual zirconium loading increased linearly with increasing amounts of zirconium used, the amount of actual zirconium loading was less than that of the zirconium used. This indicates that a considerable amount of the zirconium precursors was unreacted and was washed out during the preparation step. This is because γ -Al₂O₃ and as-synthesized Al₂O₃–ZrO₂ supports have a limited number of hydroxyl groups on the surface [22]. The Zr/Al ratio of the AZ-X supports increased linearly from 0.09 to 0.45 with increasing amount of zirconium loading from 13.4 to 38.4 wt%.

Fig. 2 shows the XRD patterns of γ -Al₂O₃ (AZ-0) and AZ-X (X = 1–4) supports calcined at 700 °C. The prepared AZ-X (X = 1–4) supports showed amorphous diffraction peaks of γ -Al₂O₃. The AZ-X (X = 1–4) supports showed diffraction peaks

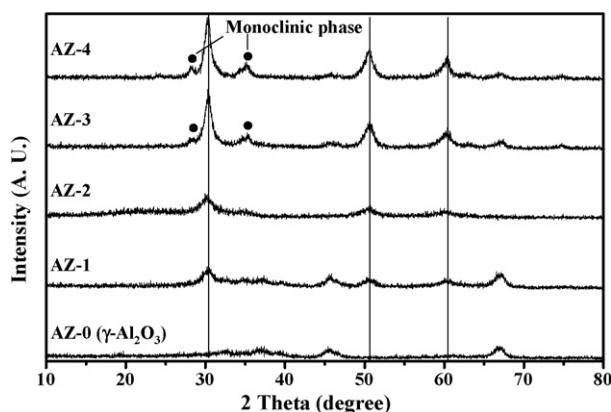


Fig. 2. XRD patterns of γ -Al₂O₃ (AZ-0) and AZ-X (X = 1–4) supports calcined at 700 °C. Solid lines represent the tetragonal phase of zirconia.

corresponding to the tetragonal phase of zirconia (solid lines in Fig. 2), which were not observed in the γ -Al₂O₃ (AZ-0) support. This result strongly supports that ZrO₂ was successfully grafted onto the γ -Al₂O₃. The AZ-1 and AZ-2 supports with low zirconium contents (Zr/Al = 0.09 and 0.17, respectively) showed relatively broad peaks corresponding to the tetragonal phase of zirconia. This indicates that zirconia was highly dispersed on the alumina in the AZ-1 and AZ-2 supports. It is believed that the co-existence of ZrO₂ and Al₂O₃ may affect the surface structure of an Al₂O₃–ZrO₂ support prepared by a grafting method, as has been observed for an Al₂O₃–ZrO₂ support prepared by a co-precipitation method [20]. Although it has been reported that the tetragonal phase of zirconia is unstable at room temperature [25], the above result may be due to the fact that meta-stable tetragonal ZrO₂ is stabilized by its incorporation into Al₂O₃ which has a higher elastic modulus than ZrO₂ [21].

On the other hand, AZ-3 and AZ-4 supports with relatively high zirconium contents (Zr/Al = 0.31 and 0.45, respectively) showed sharp peaks corresponding to the tetragonal phase of zirconia, along with weak peaks corresponding to the monoclinic phase of zirconia. The appearance of a monoclinic phase of zirconia at high zirconium loadings is believed to be due to the non-homogeneous mixing of Al and Zr species during the preparation step. It should be noted that the size of ZrO₂ particles in the AZ-3 and AZ-4 supports is larger than that in the AZ-1 and AZ-2 supports. This indicates that the grain size of ZrO₂ in the AZ-3 and AZ-4 exceeds the critical size for causing a phase transformation from the tetragonal to the monoclinic phase [21]. The above results imply that the crystalline structures of AZ-X supports are strongly influenced by the amount of zirconium grafted.

3.2. Crystalline structure of 20Ni/AZ-X (X = 0–4)

Fig. 3 shows the XRD patterns of γ -Al₂O₃ (AZ-0) and 20Ni/AZ-X (X = 0–4) catalysts calcined at 700 °C for 5 h. The 20Ni/AZ-X (X = 0–4) catalysts showed diffraction peaks for NiO species (JCPDS 22-1189) and nickel aluminate species. The co-

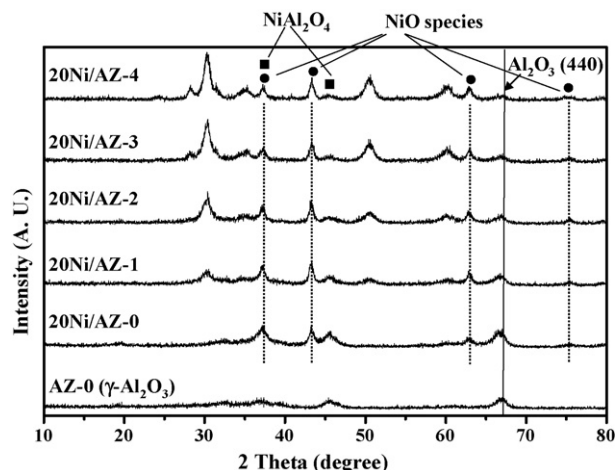


Fig. 3. XRD patterns of γ -Al₂O₃ (AZ-0) and 20Ni/AZ-X (X = 0–4) catalysts calcined at 700 °C for 5 h.

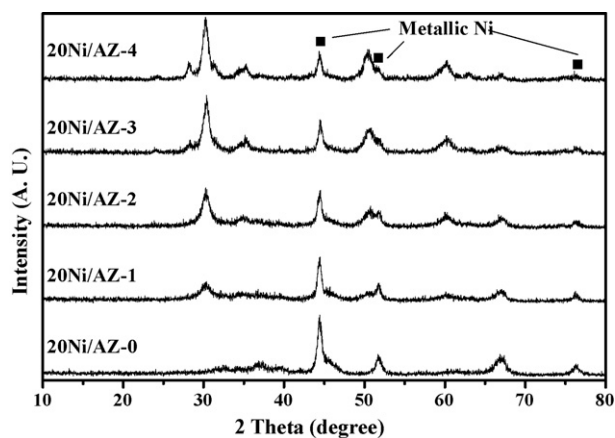


Fig. 4. XRD patterns of 20Ni/AZ- X ($X=0-4$) catalysts reduced at 800 °C for 3 h.

existence NiO and nickel aluminate (small amount) might be due to the low calcination temperature [26] or the high nickel loading. It has been reported that calcined Ni/ γ -Al₂O₃ catalysts showed no diffraction peaks for NiO species in several cases because of the strong interaction between the nickel species and alumina [26–28]. It was also reported that, since the ionic radius of nickel is larger than that of aluminum, the incorporation of nickel into the γ -Al₂O₃ increased the lattice parameter of alumina, resulting in a shift of (4 4 0) diffraction peak of alumina to a lower diffraction angle [29–32]. A shift of (4 4 0) diffraction peak of alumina to a lower diffraction angle was also observed for the 20Ni/AZ-0 catalyst. The shift of (4 4 0) diffraction peak of alumina in the 20Ni/AZ- X ($X=1-4$) catalysts became smaller or negligible with increasing amounts of zirconium grafted. This indicates that the presence of ZrO₂ inhibited the incorporation of nickel species into the lattice of γ -Al₂O₃. It also implies that the interaction between nickel species and support in the 20Ni/AZ- X ($X=1-4$) catalysts would be somewhat different from that in the 20Ni/AZ-0 catalyst.

Fig. 4 shows the XRD patterns of 20Ni/AZ- X ($X=0-4$) catalysts reduced at 800 °C for 3 h. The reduced 20Ni/AZ-0 catalyst showed relatively sharp XRD peaks corresponding to metallic nickel (JCPDS 03-1051) at $2\theta=44.8^\circ$, 52.2° , and 76.8° , indicating the formation of large nickel particles in the 20Ni/AZ-0 catalyst. On the other hand, the 20Ni/AZ- X ($X=1-4$) catalysts showed broad and weak XRD peaks for metallic nickel with increasing zirconium content. This indicates that the presence of ZrO₂ on the γ -Al₂O₃ prevented the growth of metallic nickel particles during the reduction process through the formation of a new ZrO₂-Al₂O₃ composite structure.

3.3. Reducibility of 20Ni/AZ- X ($X=0-4$)

TPR measurements were carried out to investigate the reducibility of the 20Ni/AZ- X ($X=0-4$) catalysts and to examine the interaction between nickel species and AZ- X supports. It is well known that the reduction profile of a supported nickel catalyst is dependent on the interaction between the nickel species and support. Unsupported NiO is reduced at around 400 °C, while NiO species supported on γ -Al₂O₃ is reduced at around

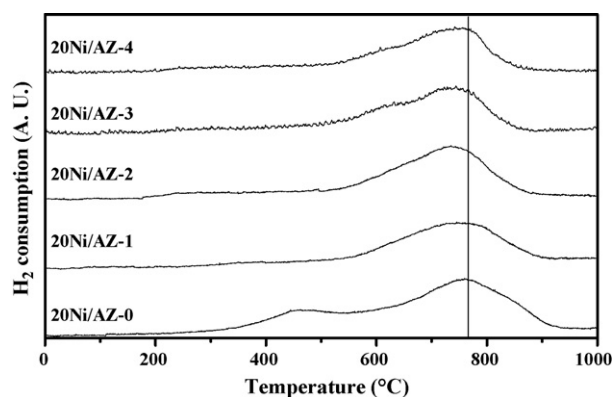


Fig. 5. TPR profiles of 20Ni/AZ- X ($X=0-4$) catalysts.

500–700 °C [28]. The reduction of nickel aluminate occurs at above 800 °C because of the strong interaction between nickel species and alumina [28].

Fig. 5 shows the TPR profiles of 20Ni/AZ- X ($X=0-4$) catalysts. The 20Ni/AZ- X ($X=1-4$) catalysts showed a broad reduction peak at around 750 °C, while 20Ni/AZ-0 catalyst showed two broad reduction peaks at around 450 and 750 °C. The reduction peak appearing at high temperature in the 20Ni/AZ-0 catalyst can be attributed to the reduction of NiO species that interacted strongly with γ -Al₂O₃ (AZ-0) and/or to the reduction of nickel aluminate species, while that appearing at low temperature is due to the reduction of NiO that interacted weakly with γ -Al₂O₃ (AZ-0). A close examination of the reduction profiles revealed that the reduction peaks of 20Ni/AZ- X ($X=1-4$) appeared at low temperature, compared to the reduction peak of 20Ni/AZ-0 which appeared at high temperature. Furthermore, no reduction peak associated with weakly interacted NiO species was observed in the 20Ni/AZ- X ($X=1-4$) catalysts due to the new interaction between Al₂O₃ and ZrO₂. Among the 20Ni/AZ- X ($X=1-4$) catalysts, the 20Ni/AZ-2 catalyst showed the highest reducibility (the lowest reduction temperature).

20Ni/AZ-3 and 20Ni/AZ-4 showed another shoulder at around 600 °C. This is believed to be due to the reduction of NiO species that had interacted with ZrO₂. This means that nickel species were supported not only on the surface of Al₂O₃ but also on the surface of ZrO₂, when much amount of ZrO₂ was grafted on the surface of the Al₂O₃. Judging from the fact that the 20Ni/AZ-2 catalyst showed the highest reducibility among the 20Ni/AZ- X ($X=1-4$) catalysts, it can be concluded that an optimum ratio of ZrO₂/Al₂O₃ is required for the efficient formation of a 20Ni/Al₂O₃-ZrO₂ catalyst.

3.4. Steam reforming of LNG over 20Ni/AZ- X ($X=0-4$) catalysts

Fig. 6 shows the LNG conversion with time on stream in the steam reforming of LNG over 20Ni/AZ- X ($X=0-4$) catalysts at 600 °C. The 20Ni/AZ- X ($X=0-4$) catalysts showed a stable catalytic performance during the catalytic reaction extending over 600 min. No significant catalyst deactivation was observed in the 20Ni/AZ- X ($X=0-4$) catalysts

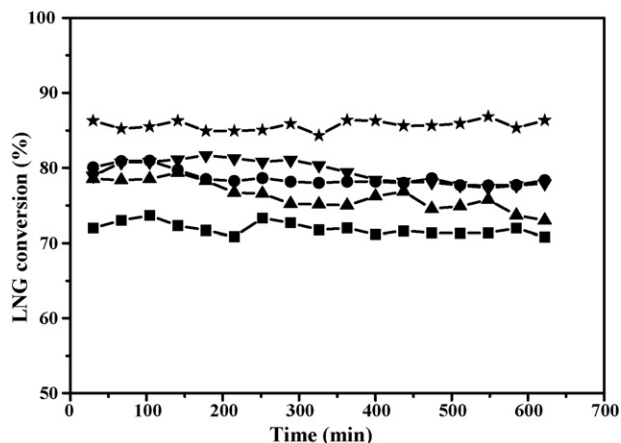


Fig. 6. LNG conversion with time on stream in the steam reforming of LNG over 20Ni/AZ- X ($X=0-4$) catalysts at 600 °C: (■) 20Ni/AZ-0; (●) 20Ni/AZ-1; (★) 20Ni/AZ-2; (▼) 20Ni/AZ-3; (▲) 20Ni/AZ-4.

due to the mild reaction conditions. LNG conversion was decreased in the order of 20Ni/AZ-2 ($Zr/Al=0.17$) > 20Ni/AZ-3 ($Zr/Al=0.31$) > 20Ni/AZ-1 ($Zr/Al=0.09$) > 20Ni/AZ-4 ($Zr/Al=0.45$) > 20Ni/AZ-0 ($Zr/Al=0$). The catalytic performance of 20Ni/AZ- X ($X=1-4$) was better than that of 20Ni/AZ-0 catalyst. Among the catalysts tested, the 20Ni/AZ-2 catalyst showed the highest LNG conversion. The reasons why the 20Ni/AZ-2 catalyst showed the best catalytic performance in this reaction can be explained by effect of zirconia grafted on the surface of the alumina. One possible reason is attributed to the high reducibility of the 20Ni/AZ-2 catalyst. Although catalyst reducibility is not the sole determining factor for catalytic performance, the 20Ni/AZ-2 catalyst showing the highest reducibility exhibited the best catalytic performance (Figs. 5 and 6). It is believed that the optimized ZrO_2/Al_2O_3 ratio of the 20Ni/AZ-2 catalyst favorably altered the interaction between the nickel species and the support, making it more suitable for the steam reforming of LNG. Another possible reason for the enhanced catalytic activity of 20Ni/AZ-2 may be due to the presence of ZrO_2 on the alumina surface. It is likely that the presence of ZrO_2 prevented the growth of metallic nickel particles during the reduction process through the formation of a $ZrO_2-Al_2O_3$ support with a favorable structure (Fig. 4).

Hydrogen production by steam reforming of methane is closely related to the following two adsorption mechanisms. One is the dissociate adsorption of methane on the active nickel surface, and the other is the dissociate adsorption of steam on the active nickel surface or support [16]. The adsorption of steam takes place competitively on the nickel and support, and zirconia is known to have a high capacity for adsorbing steam. It is believed that the zirconia in our catalyst system also played a role in enhancing the spillover of adsorbed steam from the support to the active nickel. The migrated steam, in turn, enhanced the gasification of surface hydrocarbons or carbon species, resulting in an enhanced LNG conversion and hydrogen yield. It appears that the well-developed and pure tetragonal phase of AZ-2 played an important role in the adsorption of steam and the subsequent spillover of steam from the support to the active nickel.

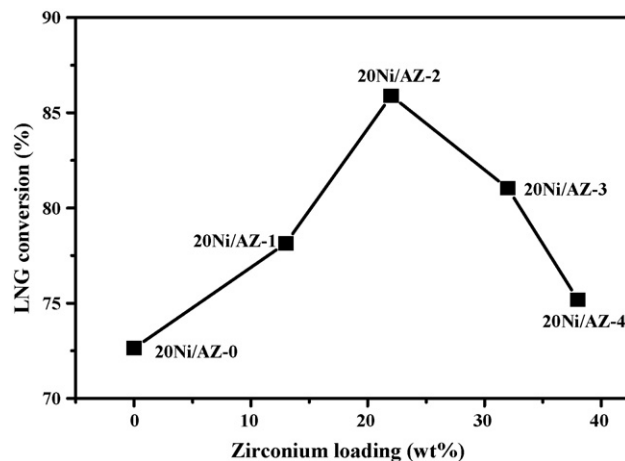


Fig. 7. LNG conversion as a function of zirconium loading over 20Ni/AZ- X ($X=0-4$) catalysts in the steam reforming of LNG at 600 °C. The data were obtained after a 300 min-reaction.

Figs. 7 and 8 show the LNG conversion and hydrogen yield as a function of zirconium loading over 20Ni/AZ- X ($X=0-4$) catalysts in the steam reforming of LNG at 600 °C, respectively. The data were obtained after a 300 min-reaction. As shown in Figs. 7 and 8, LNG conversion and hydrogen yield showed volcano-shaped curves with respect to zirconium loading. Both LNG conversion and hydrogen yield were decreased in the order of 20Ni/AZ-2 ($Zr/Al=0.17$) > 20Ni/AZ-3 ($Zr/Al=0.31$) > 20Ni/AZ-1 ($Zr/Al=0.09$) > 20Ni/AZ-4 ($Zr/Al=0.45$) > 20Ni/AZ-0 ($Zr/Al=0$). Among the catalysts tested, the 20Ni/AZ-2 catalyst showed the best catalytic performance. These results imply that an optimum ratio of ZrO_2/Al_2O_3 is required for the maximum production of hydrogen by steam reforming of LNG. It is concluded that the $Al_2O_3-ZrO_2$ (AZ- X) prepared by a grafting method served as an efficient support for the nickel catalyst in the hydrogen production by steam reforming of LNG, and that an optimum ratio of ZrO_2/Al_2O_3 was required for the maximum yield of hydrogen over 20Ni/AZ- X catalysts.

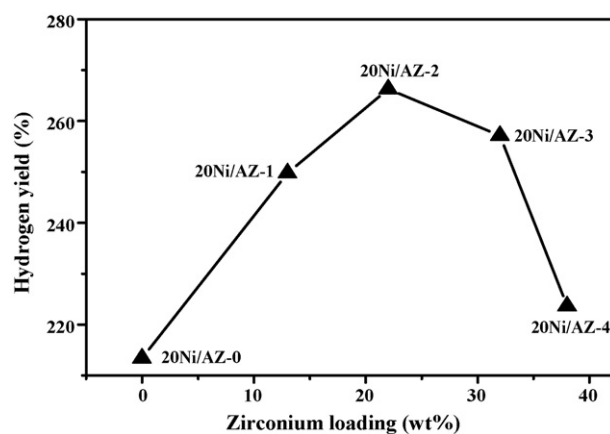


Fig. 8. Hydrogen yield as a function of zirconium loading over 20Ni/AZ- X ($X=0-4$) catalysts in the steam reforming of LNG at 600 °C. The data were obtained after a 300 min-reaction.

4. Conclusions

A series of $\text{Al}_2\text{O}_3\text{-ZrO}_2$ (AZ-*X*) supports with various zirconium loadings were prepared by grafting a zirconium precursor onto the surface of $\gamma\text{-Al}_2\text{O}_3$. Ni/ $\text{Al}_2\text{O}_3\text{-ZrO}_2$ catalysts were then prepared by an impregnation method for use in the hydrogen production by steam reforming of LNG. The effect of $\text{Al}_2\text{O}_3\text{-ZrO}_2$ supports on the performance of the Ni/ $\text{Al}_2\text{O}_3\text{-ZrO}_2$ catalysts was investigated. It was found that ZrO_2 inhibited the incorporation of nickel species into the lattice of Al_2O_3 and prevented the growth of metallic nickel particles during the reduction process through the formation of a new $\text{ZrO}_2\text{-Al}_2\text{O}_3$ composite structure. The crystalline structures and catalytic activities of the 20Ni/AZ-*X* catalysts were strongly influenced by the amount of zirconium grafted. In the hydrogen production by steam reforming of LNG, LNG conversion and hydrogen yield showed volcano-shaped curves with respect to zirconium loading. Both LNG conversion and hydrogen yield were decreased in the order of 20Ni/AZ-2 ($\text{Zr}/\text{Al}=0.17$) > 20Ni/AZ-3 ($\text{Zr}/\text{Al}=0.31$) > 20Ni/AZ-1 ($\text{Zr}/\text{Al}=0.09$) > 20Ni/AZ-4 ($\text{Zr}/\text{Al}=0.45$) > 20Ni/AZ-0 ($\text{Zr}/\text{Al}=0$). Among the catalysts tested, the 20Ni/AZ-2 catalyst showed the best catalytic performance. The well-developed and pure tetragonal phase of AZ-2 played an important role in the adsorption of steam and the subsequent spillover of steam from the support to the active nickel. It is concluded that $\text{Al}_2\text{O}_3\text{-ZrO}_2$ (AZ-*X*) prepared by a grafting method served as an efficient support for the nickel catalyst in the hydrogen production by steam reforming of LNG, and that an optimum ratio of $\text{ZrO}_2/\text{Al}_2\text{O}_3$ was required for the maximum performance of 20Ni/AZ-*X* catalysts.

Acknowledgements

The authors wish to acknowledge support from the Seoul Renewable Energy Research Consortium (Seoul R & BD Program) and RCECS (Research Center for Energy Conversion and Storage: R11-2002-102-00000-0).

References

- [1] J.N. Armor, *Appl. Catal. A* 176 (1999) 159.
 [2] S.W. Nahm, S.P. Youn, H.Y. Ha, S.-A. Hong, A.P. Maganyuk, *Korean J. Chem. Eng.* 17 (2000) 288.

- [3] K.J. Lee, D. Park, *Korean J. Chem. Eng.* 15 (1998) 658.
 [4] K.D. Ko, J.K. Lee, D. Park, S.H. Shin, *Korean J. Chem. Eng.* 12 (1995) 478.
 [5] Z.-W. Liu, K.-W. Jun, H.-S. Roh, S.-E. Park, *J. Power Sources* 111 (2002) 283.
 [6] T. Takeguchi, Y. Kani, T. Yano, R. Kikuchi, K. Eguchi, K. Tsujimoto, Y. Uchida, A. Ueno, K. Omohiki, M. Aizawa, *J. Power Sources* 112 (2002) 588.
 [7] Q. Ming, T. Healey, L. Allen, P. Irving, *Catal. Today* 77 (2002) 51.
 [8] J. Sehested, J.A.P. Gelten, I.N. Remediakis, H. Bengaard, J.K. Nørskov, *J. Catal.* 223 (2004) 432.
 [9] T. Borowiecki, G. Wojciech, D. Andrzej, *Appl. Catal. A* 270 (2004) 27.
 [10] T. Borowiecki, A. Goiebiowski, B. Stasinska, *Appl. Catal. A* 153 (1997) 141.
 [11] J.S. Lisboa, D.C.R.M. Santos, F.B. Passos, F.B. Noronha, *Catal. Today* 101 (2005) 15.
 [12] S. Natesakhawat, R.B. Watson, X. Wang, U.S. Ozkan, *J. Catal.* 234 (2005) 496.
 [13] H.-S. Roh, K.-W. Jun, S.-E. Park, *Appl. Catal. A* 251 (2003) 275.
 [14] R. Takahashi, S. Sato, T. Sodesawa, M. Yoshida, S. Tomiyama, *Appl. Catal. A* 273 (2004) 211.
 [15] M.E.S. Hegarty, A.M. O'Connor, J.R.H. Ross, *Catal. Today* 42 (1998) 225.
 [16] Y. Matsumura, T. Nakamori, *Appl. Catal. A* 258 (2004) 107.
 [17] Q.-H. Zhang, Y. Li, B.-Q. Xu, *Catal. Today* 98 (2004) 601.
 [18] M. Souza, D. Aranda, M. Schmal, *J. Catal.* 204 (2001) 498.
 [19] F. Pompeo, N.N. Nichio, O.A. Ferretti, D. Resasco, *Int. J. Hydrogen Energy* 30 (2005) 1399.
 [20] G. Li, W. Li, M. Zhang, K. Tao, *Catal. Today* 93 (2004) 595.
 [21] T. Klimova, M.L. Rojas, P. Castillo, R. Cuevas, *Micropor. Mesopor. Mater.* 20 (1998) 293.
 [22] P. Iengo, M.D. Serio, V. Solinas, D. Gazzoli, G. Salvio, E. Santacesaria, *Appl. Catal. A* 170 (1998) 225.
 [23] P. Kim, J.B. Joo, W. Kim, H. Kim, I.K. Song, J. Yi, *Carbon* 43 (2005) 2409.
 [24] M.V. Landau, E. Dafa, M.L. Kaliya, T. Sen, M. Herskowitz, *Micropor. Mesopor. Mater.* 49 (2001) 65.
 [25] T. Yamaguchi, *Catal. Today* 20 (1994) 199.
 [26] T. Ueckert, R. Lamber, N.I. Jaeger, U. Schubert, *Appl. Catal. A* 155 (1997) 75.
 [27] G. Li, L. Hu, J.M. Hill, *Appl. Catal. A* 301 (2006) 16.
 [28] M.H. Youn, J.G. Seo, P. Kim, I.K. Song, *J. Mol. Catal. A* 261 (2007) 276.
 [29] P. Kim, Y. Kim, H. Kim, I.K. Song, J. Yi, *Appl. Catal. A* 272 (2004) 157.
 [30] E.D. Dimotakis, T.J. Pinnavaia, *Inorg. Chem.* 29 (1990) 2393.
 [31] A. Corma, V. Fornes, R.M. Aranda, F. Rey, *J. Catal.* 134 (1992) 58.
 [32] J.A. Wang, A. Morales, X. Bokhimi, O. Novaro, *Chem. Mater.* 11 (1999) 308.